Rev. Roum. Sci. Techn.– Électrotechn. et Énerg.
Vol. **64**, *1*, pp. 51–56, Bucarest, 2019

Électronique et transmission de l'information

DECOUPLED ACTIVE AND REACTIVE POWER CONTROL STRATEGY OF GRID-CONNECTED SIX-LEVEL DIODE-CLAMPED INVERTERS BASED ON FINITE SET MODEL PREDICTIVE CONTROL FOR PHOTOVOLTAIC APPLICATION

ABDELBASET LAIB[1], FATEH KRIM[1], BILLEL TALBI[1], HAMZA FEROURA[1], ABBES KIHAL[1]

Key words: Solar energy, Six-level neutral point clamping (NPC) inverter, Decoupled active and reactive power control, Finite set model predictive control.

In this paper, a decoupled active and reactive power control strategy based on finite set model predictive control is proposed to control grid connected six-level NPC inverters for photovoltaic application. The purposes of this strategy are: injection control of the active power produced by photovoltaic system as well as the reactive power requested by the grid operator, also the assurance of high grid current quality and dc link capacitors voltages balance. Using the discrete time model of six level NPC inverter tied to the network, the proposed strategy is based on prediction of the future behavior of active and reactive grid power values and dc link capacitor voltages for 216 possible switching states and compare them with using a cost function for obtaining the optimal vector and applying it during the next sampling time. The global system is simulated using Matlab/Simulink and Simpower system packages. The performance of the proposed strategy is evaluated under the step change in the solar irradiation and the reactive power reference. The obtained results proves that the proposed strategy provide high performance control.

1. INTRODUCTION

Recently, the increased energy consumption and environmental problems are the greatest challenges facing the world. Renewable energy sources were emerged like the suitable solution for avoiding these problems due to their advantages (clean and sustainable source energy) [1–3]. Solar energy is considered as the most renewable energy source used in the world due to easier to be harvested, converted, and delivered to the grid by a variety of power converters. However, it suffers from several problems to adapt this energy to the public grid [4]. Grid connected photovoltaic (PV) systems have been used to inject the energy produced by the PV arrays into the network [4]. Among the current objective of these systems is to inject the produced PV power into the network in addition to the reactive power requested by the grid operator with high grid current quality under climatic changes.

Nevertheless, the use of multilevel NPC inverters provides high performance control in terms of powers control and high grid currents quality. Moreover, they are suitable for high-power grid-tied inverter systems [5], where they use the semiconductor switches connected in series, which allow the operation at higher dc voltages. However, they possess major problems which are the unbalancing capacitor potential of dc link voltage and the complexity of control design. These problems limit the utilization of these inverters.

Several classical power control methods are proposed and applied in the literature to the high level NPC grid connected inverter. These methods can be divided in two categories:

- Power control methods without modulation stage such as: direct power control (DPC) [6, 7] and virtual flux oriented DPC (F-DPC) [8] based on switching table. The design of switching table will be complex in high level inverter cases (3 level and more). Furthermore, these methods do not provide high preference power control.
- Power control methods with modulation stage such as: voltage-oriented control (VOC) [9], voltage-based direct power control (V-DPC) [10, 11], Virtual flux oriented control [9]. To apply these techniques, proportional integral (PI) controller is necessary in the internal current loop in addition to modulation stage as pulse width modulation (PWM) or space-vector modulation (SVM) [12, 13]. To design the modulation stage in high level inverter, the dc link capacitor voltages control must be included which makes it more complicated. Moreover, a PI controller drawbacks and control delay will reduce the performance.

In recent research, the finite-control set model predictive control (FCS-MPC) has been applied in many power electronics applications [12–17]. This technique is easily designed and does not need PI controllers and modulation stage. In grid connected systems, FCS-MPC method is employed for different control purposes such as grid current control [14], d-q rotating frame grid current control [12] and power control [13]. FCS-MPC is considered as a good and simple control for high level inverter NPC, where it is easy to include the dc link capacitor voltages balancing in the objective control. Furthermore, it provides high performance control in comparison with classical methods [12–14]. Moreover, different researches have employed this method with multilevel NPC inverters for the production of renewable power as: [12, 13] with four level NPC inverter, [17] with three level inverter, but the application to converters with higher level (more than five level) has not been investigated.

In order to employ higher level NPC inverter (six level) in grid PV systems with simple control design, this paper proposes a decoupled active and reactive power control strategy based on finite set model predictive control. To evaluate the proposed control scheme, different tests under sudden irradiation changes and reactive power requested by the grid operator changes are performed by numerical simulation through Matlab/Simulink package. The power

[1] LEPCI laboratory, Electronics dept. Setif-1 University, Route Bejaia, Sétif, Algeria, E-mail: laibabdelbasset42@gmail.com

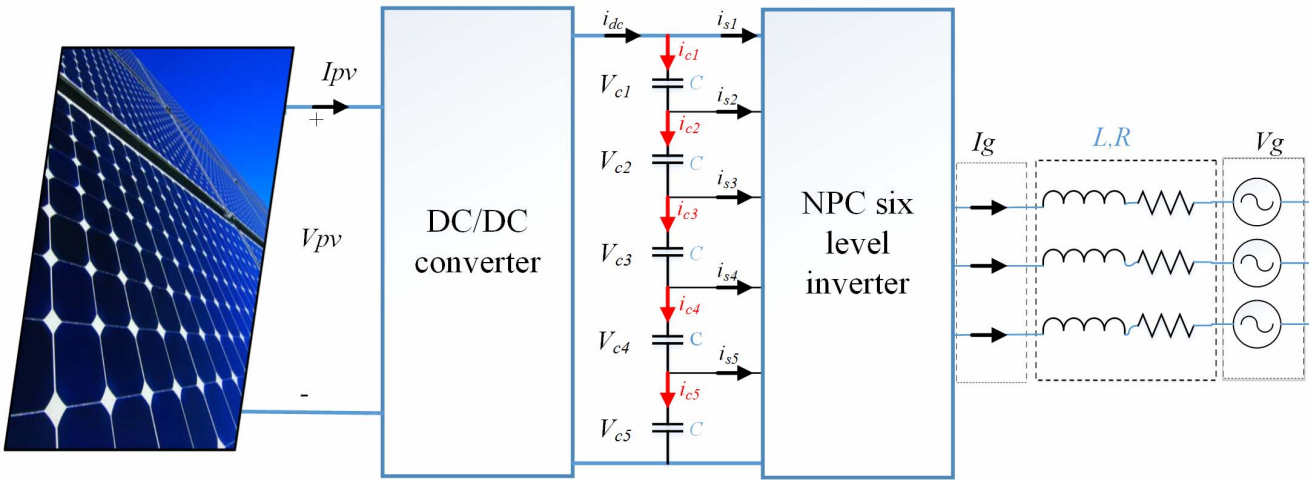

Fig. 1 – System global configuration.

control and dc link capacitor voltages balancing are observed and evaluated in transient and steady states under irradiation and reactive power reference changes. Also, the grid current quality is in compliance with international standards (IEEE-519) for all irradiation and reactive power levels.

This paper is organized as follows. In Section 2, the proposed global system is presented, while, in the Section 3, the control of global system is discussed. In Section 4, the decoupled active and reactive power control for six level inverter is introduced. The simulation results are discussed in Section 5, and finally, in Section 6, conclusions are drawn.

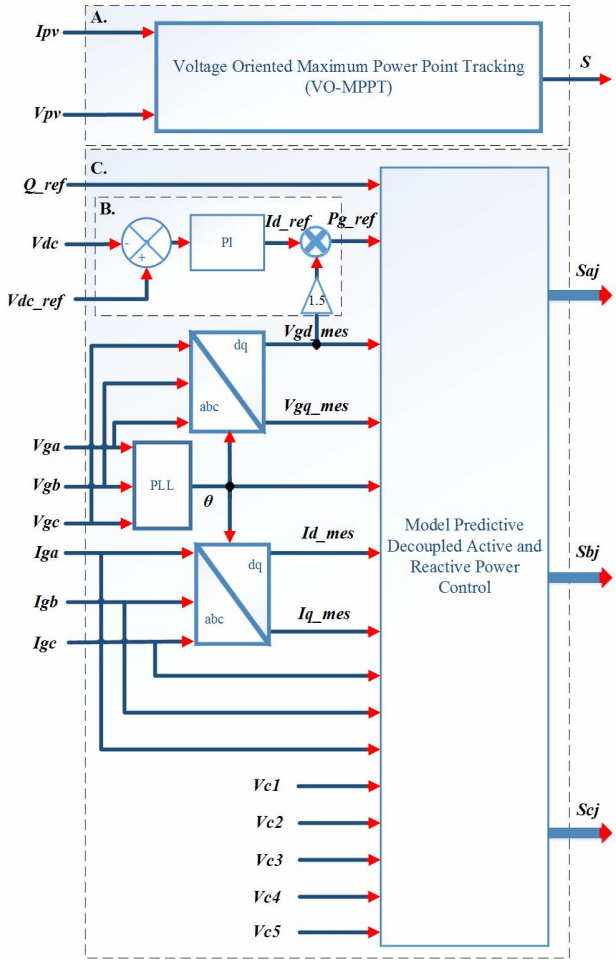

Fig. 2 – System global control.

2. SYSTEM GLOBAL CONFIGURATION

This paper concerns the application of high level NPC inverter in PV systems. Where, as illustrated in Fig. 1, the system studied consist of PV array, dc/dc converter (boost), six-level NPC inverter, and R , L filter tied to the grid .

The PV array generates the power depending on solar radiations. The boost converter is used to track the maximum power point (MPP) and to deliver it continuously to the dc link. The six-level NPC inverter injects the power coming from the boost to the grid tacking into account reactive power demanded by grid operator.

3. SYSTEM GLOBAL CONTROL

As shown in Fig. 2, the proposed system is controlled with a three steps technique:

A) A voltage oriented maximum power point tracking (MPPT) based on PI controller used in [2] as conventional method is employed to track the maximum power point delivered by the PV system under irradiation change.

B) A simple PI with gains ($K_i = -3.5$, $K_p = -0.5$) is used to control the dc link voltage and generate the active power reference.

C) Decoupled active and reactive power control strategy for grid-connected based on finite set Model predictive control is proposed for six-level diode-clamped inverters. This method is under consideration in this paper.

4. DECOUPLED ACTIVE AND REACTIVE POWER CONTROL STRATEGY BASED ON FINITE SET MODEL PREDICTIVE CONTROL

To inject the high produced PV power in addition to reactive power as per the grid operator request with high performance, a high level NPC inverter (six level) is employed for this reason. The six level NPC converter generates six voltage levels. These levels are achieved through the switching states summarized in the Table 1. The three phase six level NPC inverter has a total of 216 possible switching states.

Depending on the classic model predictive control (MPC) proposed in [14–16], a decoupled active and reactive -control is proposed and applied to PV system

using six level NPC inverter. The aims of the proposed control scheme are:

- Enforce P_g to track the P_{g_ref} delivered by the dc link voltage control.
- Enforce Q_g to track the Q_{gref} demanded by the grid operator.
- Assure the balance of five dc link capacitor voltages.

Those goals are included in the cost function g which is defined as:

$$g = \left|P_{g\_ref} - P_g(k+1)\right| + \left|Q_{g\_ref} - Q_g(k+1)\right| + \lambda\begin{bmatrix} \sum_{j=1}^{4}\left|V_{cj}(k+1) - V_{cj+1}(k+1)\right| + \\ \sum_{j=1}^{3}\left|V_{cj}(k+1) - V_{cj+2}(k+1)\right| + \\ \sum_{j=1}^{2}\left|V_{cj}(k+1) - V_{cj+3}(k+1)\right| + \\ \left|V_{c1}(k+1) - V_{c5}(k+1)\right| \end{bmatrix}, \quad (1)$$

where P_{g_ref} is the power active reference delivered by DC-link control.

Q_{g_ref} is the reactive power reference demanded by the grid operator.

The $P_g(k+1)$, $Q_g(k+1)$,$V_{cj}(k+1)$ are the future behavior of active power, reactive power and dc link capacitor voltage number j respectively, whose calculation are detailed in the next subsections.

λ is the weight factor of the dc link capacitor voltages balance.

More details about the functionality of the proposed control is given in sub-section 4.3.

4.1. FUTURE ACTIVE AND REACTIVE POWER CALCULATION

For calculating the future active and reactive powers, the mathematical model of six level NPC tied to the grid through *LR* filter is necessary. It is expressed by the following equation [14]

$$\frac{\mathrm{d}i_g(t)}{\mathrm{d}t} = \frac{1}{L}\left[V - v_g(t) - \mathrm{R}i_g(t)\right] , \quad (2)$$

where i_g and v_g are the measured grid current and voltage respectively.

The above expression can be rewritten in synchronous frame as fellows [12]

$$\begin{cases} \dfrac{\mathrm{d}i_d(t)}{\mathrm{d}t} - \omega i_q(t) = \dfrac{1}{L}\left[-\mathrm{R}i_d(t) - v_{gd}(t) + V_d\right] \\ \dfrac{\mathrm{d}i_q(t)}{\mathrm{d}t} + \omega i_d(t) = \dfrac{1}{L}\left[-\mathrm{R}i_q(t) - v_{gq}(t) + V_q\right] \end{cases}, \quad (3)$$

where V_d and V_q represent the voltage vectors generated by the inverter in rotating axis d-q, which can be obtained by the conversion of voltage vectors in stationary frame to rotating frame. While, ω is the grid angular frequency.

By using the Euler forward method [14], the discrete time model of Eq. (7) yields

$$\begin{cases} i_d(k+1) = \dfrac{\mathrm{T_s}}{\mathrm{L}}\left[-\mathrm{R}i_d(k) - v_{gd}(k) + V_d(k)\right] + \\ \qquad \mathrm{T_s}\omega i_q(k) + i_d(k) \\ i_q(k+1) = \dfrac{\mathrm{T_s}}{\mathrm{L}}\left[-\mathrm{R}i_q(k) - v_{gq}(k) + V_q(k)\right] - \\ \qquad \mathrm{T_s}\omega i_d(k) + i_q(k) \end{cases} \quad (4)$$

Where T_s is the sampling time.

From Eq. 4, the future behavior of active and reactive powers can be written as:

$$\begin{cases} P_g(k+1) = 1.5 v_{gd}(k) i_{gd}(k+1) \\ Q_g(k+1) = 1.5 v_{gd}(k) i_{gq}(k+1) \end{cases} \quad (5)$$

4.2. FUTURE BEHAVIOR OF DC LINK CAPACITOR VOLTAGES

The calculation of future behavior of DC-link capacitor voltages is based on DC-link capacitors model which can be expressed as [15]

$$\frac{\mathrm{d}V_{cj}(t)}{\mathrm{d}t} = \frac{1}{\mathrm{C}} i_{cj}(t) , \quad (6)$$

where V_{cj} and i_{cj} are the voltage and current of capacitor number j respectively.

The discrete time model of Eq. (6) is given as [15]

$$V_{cj}(k+1) = V_{cj}(k) + \frac{T_s}{C} i_{cj}(k) . \quad (7)$$

As illustrated in Fig.1, the capacitor currents can be derived in terms of the net dc current i_{dc} and the input inverter currents i_{sj} as fellows

$$\begin{cases} i_{c1} = i_{dc} - i_{s1} \\ i_{c2} = i_{dc} + i_{c1} - i_{s2} \\ i_{c3} = i_{dc} + i_{c2} - i_{s3} \\ i_{c4} = i_{dc} + i_{c3} - i_{s4} \\ i_{c5} = i_{dc} + i_{c4} - i_{s5} \end{cases} . \quad (8)$$

The i_{dc} becomes null under equal energy among the capacitors condition and Eq. (8) can be rewritten as [12]

$$\begin{cases} i_{c1} = -i_{s1} \\ i_{c2} = i_{c1} - i_{s2} \\ i_{c3} = i_{c2} - i_{s3} \\ i_{c4} = i_{c3} - i_{s4} \\ i_{c5} = i_{c4} - i_{s5} \end{cases} . \quad (9)$$

The inverter input currents can be estimated from the measured grid currents (i_{ga}, i_{gb}, and i_{gc}) as follows

Table 1
Switching states for one phase of six level inverter NPC

voltage levels	Switching state									
	S_{1x}	S_{2x}	S_{3x}	S_{4x}	S_{5x}	S_{6x}	S_{7x}	S_{8x}	S_{9x}	S_{10x}
Vdc	1	1	1	1	1	0	0	0	0	0
4Vdc/5	0	1	1	1	1	1	0	0	0	0
3Vdc/5	0	0	1	1	1	1	1	0	0	0
2Vdc/5	0	0	0	1	1	1	1	1	0	0
Vdc/5	0	0	0	0	1	1	1	1	1	0
0	0	0	0	0	0	1	1	1	1	1

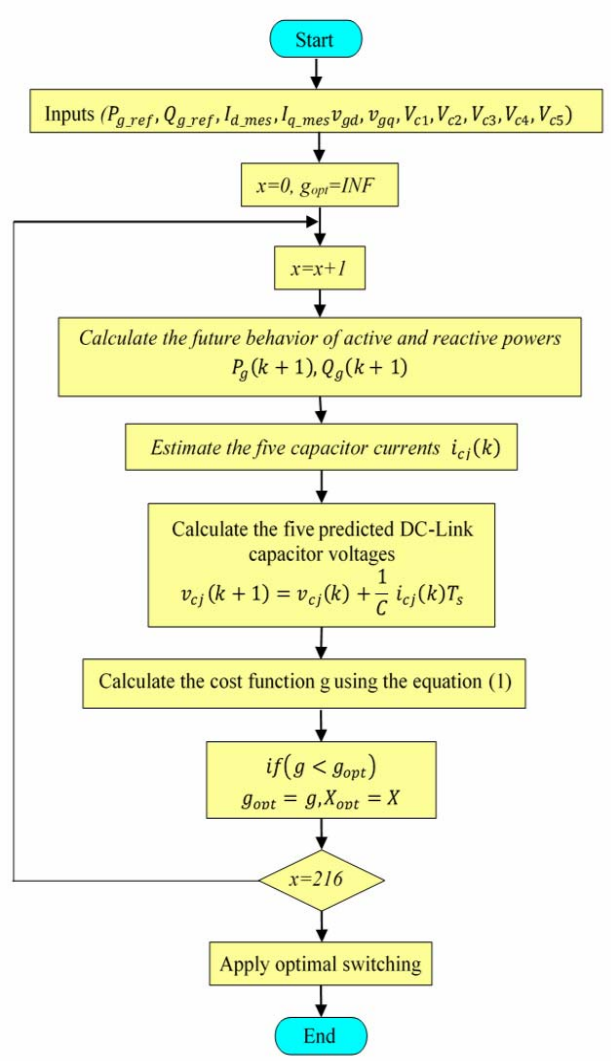

Fig. 3 – Flowchart of the proposed control.

$$\begin{cases} i_{s1} = \sum_{x=a,b,c} (S_x = 1) i_{xg} \\ i_{s2} = \sum_{x=a,b,c} (S_x = 2) i_{xg} \\ i_{s3} = \sum_{x=a,b,c} (S_x = 3) i_{xg} \\ i_{s4} = \sum_{x=a,b,c} (S_x = 4) i_{xg} \\ i_{s5} = \sum_{x=a,b,c} (S_x = 5) i_{xg} \end{cases} \quad (10)$$

4.3. CONTROL STRATEGY

From the measured grid currents and voltages in addition to the five dc link capacitor voltages, the future behaviors of active power, reactive power and dc link capacitor voltages are calculated for all 216 possible switching states. Then, a cost function g is evaluated for all switching states. The switching state that minimizes the cost function is selected for applying during the next sampling time. The flowchart presented in Fig. 3 summarizes the operating of the proposed method.

5. SIMULATION RESULTS

To substantiate the functionality of the proposed control scheme under solar irradiation and reactive power reference variations, a numerical simulation is carried out through Matlab/ Simulink packages with the parameters detailed in Table 2.

In order to test the proposed method in transit state, different sudden changes of the solar irradiation and reactive power reference are considered, as presented in Fig 4a and Fig. 4f, respectively.

Firstly, a sudden decrease in the solar irradiation from 1000 to 400 W/m² at instant 0.6 s is occurred. It is clearly seen that the PV system reaches rapidly achieved the new MPP. In addition, this change leads to undershoot and small rising time in V_{dc} over its reference as shown in Fig. 4c. Despite that, the active and reactive powers track their references very well and the capacitor voltages are well balanced as illustrated in Figs. 4e, f, g, whereas the grid currents decreased and remain sinusoidal.

Then, a sudden increase in the solar irradiation from 400 to 800 W/m² at instant 1.4 s is performed, which leads to increase the PV power output. As presented in Fig. 4b, the PV system continuously tracked the MPP. Moreover, the increase in the irradiance level leads to overshoot and small stilling time in V_{dc} over its reference as shown in Fig. 4c. Even though, as shown in Fig. 4f and Fig. 4g, the active and reactive powers track their references smoothly. In addition, as presented in Fig. 4d, the five dc link capacitor voltages are kept up in balance, as well as, the grid currents are increased and kept sinusoidal.

Next, a step decrease in the reactive power reference from 0 var to –0.15 Mvar at instant 2 s is occurred. The PV power output remained fixed due to non-change in solar irradiation. As results, a small deviation in V_{dc} over its reference is observed as illustrated in Fig. 4c. The reactive power tracks its reference quickly (during 1.2 ms). Furthermore, the balance of dc link capacitor voltage is achieved. Whereas the grid currents change the angle as showed in Fig. 5a and increase rapidly due to the increase in grid apparent power S_g, where the grid current amplitude

Table 2

System global parameters

PV Siemens SM110 electrical parameters	**Value**
Maximum power (*Pmpp*)	120 W
Open circuit voltage (*Voc*)	42.1 V
Short circuit current (*Isc*)	3.87 A
Voltage at *Pmax*	*33.7*
current at Pmax	*3.56*
Number of cells connected in parallel (*N*p)	1
Number of cells connected in series (*N*s)	72
Number of modules connected in series (*N*ss)	36
Number of modules connected in parallel (*N*pp)	36
Boost converter electrical parameters	**Value**
Input capacitor *Cin*	550 µF
Inductor *L*	1 mH
Dc link capacitors value *C*	2200 µF
Grid electrical parameters	**Value**
Grid inductance *L*	10 mH
Grid resistance *R*	0.1 Ω
Grid Peak Voltage *Vg*	500 V
Grid frequency *Fg*	50 Hz
Simulation Parameters	**Value**
MPPT sampling time *Tm*	1 ms
Predictive sampling time *Ts*	0.1 ms

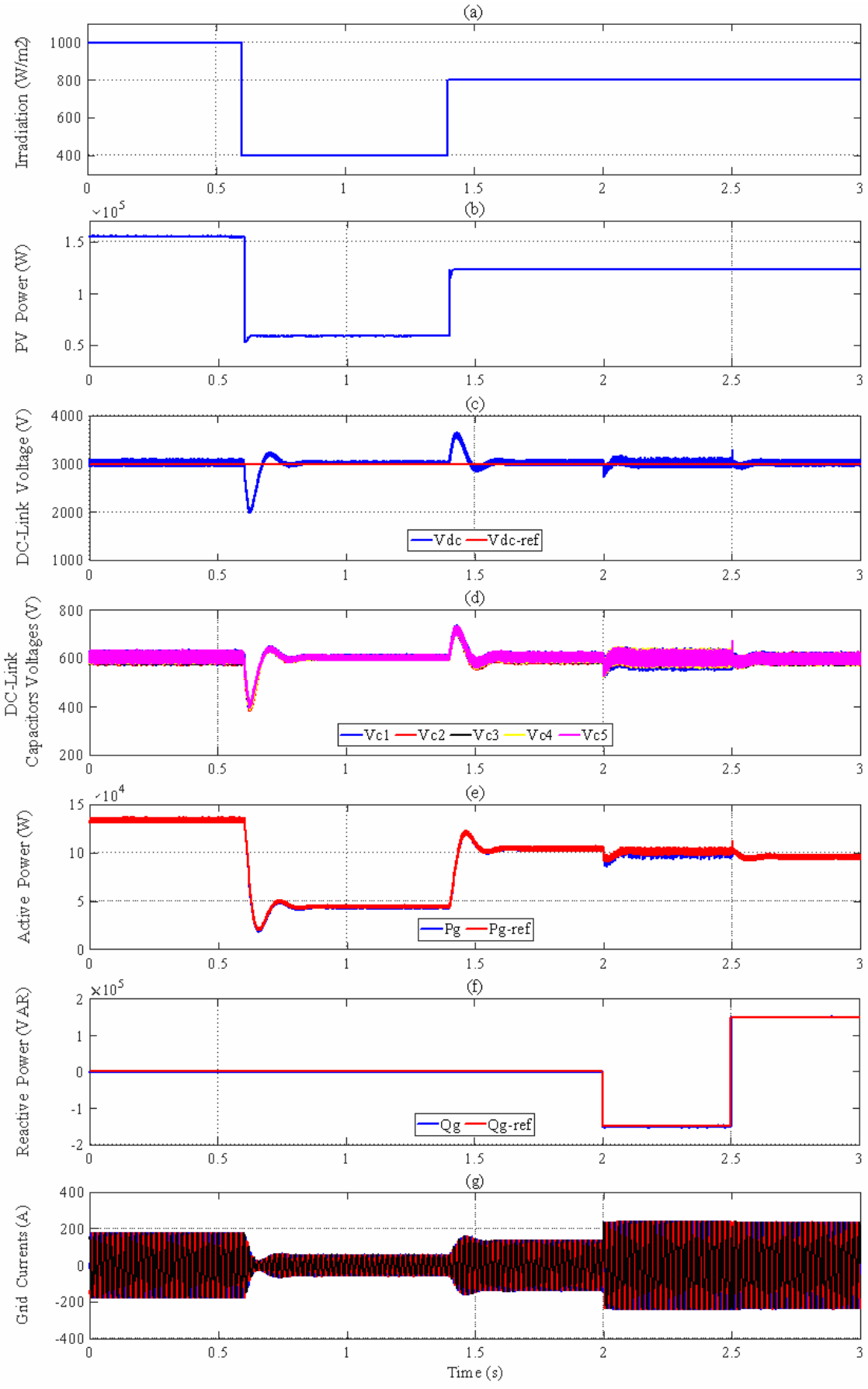

Fig. 4 – Simulation results: test of global system under solar irradiation and reactive power reference change.

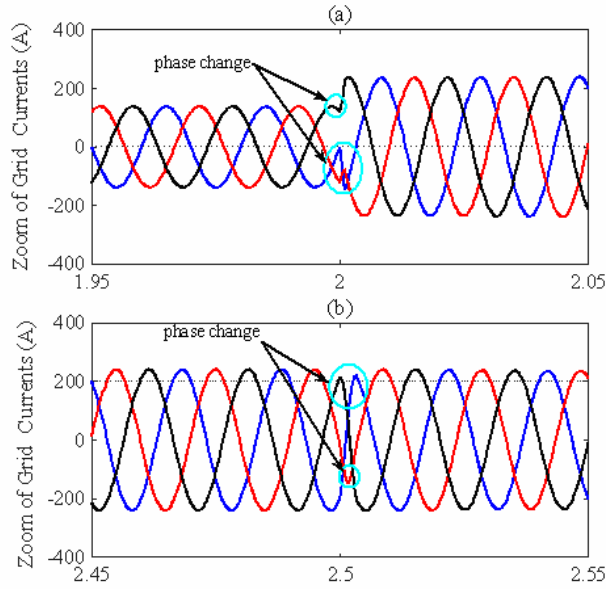

Fig. 5 – Phase change in grid currents under reactive power reference change.

is proportional to S_g.

Finally, at instant 2.5 s, a large step increase in the reactive power reference from –0.15 Mvar to 0.15 Mvar is occurred. This leads to small deviation in V_{dc} over its reference. The reactive power tracks its reference rapidly during 3 ms, whereas the five voltage capacitors are maintained in balance, the grid currents change the angle with keeping the sinusoidal form as showed in Fig. 5b.

As shown in Fig. 4, the proposed controller provides high performance during five steady-state operating conditions, where the active and reactive powers are completely regulated to their references as presented in Figs. 4f and g. Moreover, as shown in Fig. 4c, and Fig. 4h, the five dc link capacitor voltages are in perfect balancing and the grid currents are balanced and sinusoidal.

The proposed control scheme provides high grid current quality under all solar irradiation and reactive power reference levels according to the international standards (IEEE-519, THD < 5 %), as presented in Table 3.

Table 3
THD under different irradiation reactive power reference levels

Level	1000 W/m²	400 W/m²	800 W/m²	-0.15 MVAR	+0.15 MVAR
THD %	0.63	1.36	0.62	1.12	0.46

6. CONCLUSIONS

This paper addressed the decoupled active and reactive power control strategy based on finite set model predictive control applied to grid connected six-level NPC inverter for photovoltaic application. The simulation results obtained by using Matlab/Simulink and Simpower system packages prove that the proposed strategy achieved high performance in power control and perfect dc link capacitor voltages balance under sudden change and steady-state operating conditions in the solar irradiation and reactive power reference. Moreover, high grid current quality at different solar irradiation and reactive power reference levels in accordance with international standards (IEEE-519) has been achieved.

Received on October 20, 2018

REFERENCES

1. B. Bendib, H. Belmili, F. Krim, *A survey of the most used MPPT methods: Conventional and advanced algorithms applied for photovoltaic systems*, Renew. Sustain. Energy Rev. **45**, p. 637-648 2015.
2. A. Kihel, F. Krim, A. Laib, *MPPT voltage oriented loop based on integral sliding mode control applied to the boost converter*, In: 6th International Conference on Systems and Control (ICSC), Batna, Algeria: IEEE. pp. 205-209, 2017.
3. B. Talbi, F. Krim, T. Rekioua, A. Laib, H. Feroura, *Design and hardware validation of modified P&O algorithm by fuzzy logic approach based on model predictive control for MPPT of PV systems*. J. Renew. Sustain. Energy., **9**, *4*, p. 043503, 2017.
4. S. Bouchakour, A. Tahour, H. Sayah ,K. Abdeladim, A. Abdelghani, *Direct Power Control of Grid Connected Photovoltaic System with Linear Reoriented Coordinate Method as Maximum Power Point Tracking Algorithm,* Rev. Roum. Sci. Techn. – Électrotechn. et Énerg., **59**, *1*, p. 57–66, 2014.
5. M. Flitti, M. K. Fellah, M. Yaichi, M. khatir, M. F. Benkhoris, *Control design of statcom using five level neutral point clamped converter and its application to reactive power,* Rev. Roum. Sci. Techn. – Électrotechn. et Énerg., **59**, *4*, pp. 351–360, 2014.
6. S. Rivera, S. Kouro, B. Wu, S. Alepuz, M. Malinowski, P. Cortes, J. Rodriguez, Multilevel direct power control—A generalized approach for grid-tied multilevel converter applications, IEEE Transactions on Power Electronics, 29, 10, 5592-5604, 2014.
7. J. Eloy-Garcia, S. Arnaltes, J. L. Rodriguez-Amenedo, *Extended direct power control for multilevel inverters including DC link middle point voltage control*, IET Electric Power Applications, **1**, *4*, p. 571-580, 2007.
8. L. A. Serpa, P. M. Barbosa, P. K. Steimer, J. W. Kolar, *Five-level virtual-flux direct power control for the active neutral-point clamped multilevel inverter*, In Power Electronics Specialists Conference, PESC 2008, Rhodes, Greece: IEEE, pp. 1668-1674, 2008.
9. B.Wu, Y. Lang, N. Zargari, S. Kouro, *Power Conversion and Control of Wind Energy Systems*, John Wiley & Sons, 2011.
10. O. Aouchenni, R. Babouri, K. Ghedamsi, D. Aouzellag, *Wind farm based on doubly fed induction generator entirely interfaced with power grid through multilevel inverter*, Rev. Roum. Sci. Techn. – Électrotechn. et Énerg., **62**, *2*, pp. 170–174, 2017.
11. R. Portillo, S. Vazquez, J. I. Leon, M. M. Prats, L. G. Franquelo, *Model based adaptive direct power control for three-level NPC converters*, IEEE Transactions on Industrial Informatics, **9,** *2*, pp. 1148-1157, 2013.
12. V. Yaramasu, B. Wu, J. Chen, *Model-Predictive Control of Grid-Tied Four-Level Diode-Clamped Inverters for High-Power Wind Energy Conversion Systems,* IEEE transactions on power electronics, **29**, *6*, p. 2861-2873, 2014.
13. V. Yaramasu, B. Wu, *Model Predictive Decoupled Active and Reactive Power Control for High-Power Grid-Connected Four-Level Diode-Clamped Inverters,* IEEE Transactions on Industrial Electronics, **61**, *7*, 3407-3416,2014.
14. J. Rodriguez, J. Pontt, C. A. Silva, P. Correa, P. Lezana, P. Cortés, U. Ammann, *Predictive current control of a voltage source inverter*, IEEE Trans. Ind. Electron. **54**, *1*, p. 495-503, 2007.
15. R. Vargas, P. Cortés, U. Ammann, J. Rodríguez, J. Pontt, *Predictive control of a three-phase neutral-point-clamped inverter*, IEEE Trans. Ind. Electron. **54**, *5*, pp. 2697-2705, 2007.
16. J. Rodriguez, P. Cortes, Predictive control of power converters and electrical drives ,John Wiley & Sons, **40**, pp. 65-79, 2012.
17. A. K. Bonala, S. R. Sandepudi, V. P. Muddineni, *Model predictive current control with modified synchronous detection technique for three-phase 3L-NPC multi-functional solar photovoltaic system*. In IEEE International Conference on Power Electronics, Drives and Energy Systems (PEDES), Trivandrum, India, pp. 1-6, 2016.